Novel Series of ^{111}In-Labeled Bombesin Analogs as Potential Radiopharmaceuticals for Specific Targeting of Gastrin-Releasing Peptide Receptors Expressed on Human Prostate Cancer Cells

Timothy J. Hoffman, PhD[1,2]; Hariprasad Gali, PhD[3]; C. Jeffrey Smith, PhD[3]; Gary L. Sieckman, BS[1]; Donald L. Hayes, BS[3]; Nellie K. Owen, DVM[3]; and Wynn A. Volkert, PhD[1,3]

[1]Research Service, Harry S. Truman Memorial VA Hospital, Columbia, Missouri; [2]Department of Internal Medicine, University of Missouri-Columbia School of Medicine, Columbia, Missouri; and [3]Department of Radiology, University of Missouri-Columbia School of Medicine, Columbia, Missouri

Gastrin-releasing peptide (GRP) receptors have been shown to be expressed with high densities on several types of cancer cells including prostate, breast, small cell lung, and pancreas cancers. Bombesin (BBN) has been known to bind to GRP receptors with high affinity and specificity. The aim of these studies was to develop new ^{111}In-labeled BBN analogs having high tumor uptake and optimal pharmacokinetics for specific targeting of human prostate cancers. **Methods:** A novel series of dodecanetetraacetic acid (DOTA)-X-BBN[7–14]NH_2 (X = 0, β-Ala, 5-Ava, 8-Aoc, or 11-Aun) conjugates and their In(III)/^{111}In complexes exhibiting high GRP-receptor–binding affinities were synthesized and characterized. **Results:** In vitro competitive binding assays, using PC-3 androgen-independent human prostate cancer cells, demonstrated values of <2.5 nmol/L for inhibitory concentration of 50% for analogs with β-Ala, 5-Ava, and 8-Aoc spacers. In vivo biodistribution studies of the ^{111}In-DOTA-X-BBN[7–14]NH_2 conjugates performed on CF-1 mice at 1 h after injection have revealed that the uptake of radioactivity in the pancreas, a GRP-receptor–expressing tissue, increased as a function of hydrocarbon spacer length (i.e., from 0.20 ± 0.04 percentage injected dose [%ID] per gram for the analog with no spacer to a maximum of 26.97 ± 3.97 %ID/g for the analog with 8-Aoc spacer). The radioactivity was cleared efficiently from the blood pool by excretion mainly through the renal/urinary pathway (e.g., 71.6 ± 1.8 %ID at 1 h after injection for 8-Aoc spacer analog). In vivo pharmacokinetic studies of the ^{111}In-DOTA-8-Aoc-BBN[7–14]NH_2 conjugate conducted on PC-3 human prostate cancer–derived xenografts in SCID mice showed a specific uptake of radioactivity in tumor, with 3.63 ± 1.11 %ID/g observed at 1 h after injection. High tumor-to-blood and tumor-to-muscle ratios of approximately 6:1 and 45:1, respectively, were achieved at 1 h after injection. Relative to the radioactivity observed in the tumor at 1 h after injection, 43%, 19%, and 9% of the radioactivity was retained at, respectively, 24, 48, and 72 h after injection. **Conclusion:** These studies showed that radiometallated DOTA-X-BBN[7–14]NH_2 constructs with hydrocarbon spacers ranging from 5 to 8 carbon atoms are feasible candidates for further development as diagnostic and therapeutic radiopharmaceuticals for patients with GRP-positive cancers.

Key Words: gastrin-releasing peptide; bombesin; ^{111}In; prostate cancer

J Nucl Med 2003; 44:823–831

Radiolabeled small receptor-avid peptides have attracted considerable interest because of their wide applicability in the development of target-specific radiopharmaceuticals (*1*,*2*). Several malignant tumors overexpress certain types of receptors on their surface that make the tumors potential targets for imaging and therapy with radiolabeled receptor-avid peptides (*1*,*2*). Bombesin (BBN), a 14-amino-acid peptide, is an amphibian analog of human gastrin-releasing peptide (GRP) that binds with high affinity and specificity to the GRP-receptor subtype (BB2) of the BBN-receptor family (*3*,*4*). GRP receptors have been shown to be expressed with high densities on several types of cancer cells including prostate, breast, small cell lung, and pancreas cancers (*5*–*7*). Many synthetic BBN peptide antagonists that bind with high affinities to GRP receptors have been synthesized to evaluate their potential to reduce or minimize the rate of growth of GRP-receptor–expressing cancers (*3*–*8*). Insights from this research guide the design of radiolabeled BBN conjugates that maintain high in vitro and in vivo GRP-receptor–binding affinities.

Significant progress has been made over the past few years in developing effective strategies to produce radiolabeled BBN analogs that specifically target GRP-receptor–expressing cancer cells in vitro and in vivo (*9*–*24*). Our laboratory has focused on developing radiometallated BBN analogs in which radiometal chelates are linked to the

Received Jun. 17, 2002; revision accepted Nov. 27, 2002.

For correspondence or reprints contact: Wynn A. Volkert, PhD, Radiopharmaceutical Sciences Institute, 143 Major Hall, DC200.0 HSC, University of Missouri-Columbia, Columbia, MO 65212.

E-mail: VolkertW@health.missouri.edu

truncated BBN[7–14]NH_2 sequence that serves as the highly specific GRP-receptor–binding motif (*2,12–18*). Use of this truncated BBN[7–14]NH_2 sequence was selected since the BBN derivatives containing this sequence have been shown to bind in an agonist manner to the GRP receptors (*7,14,17*). As with other G-protein–coupled, 7-transmembrane segment (7-TMS) receptors, specific binding of an agonist to cell-surface GRP receptors typically leads to internalization of the agonist–receptor complex (*25–27*), providing an effective method to produce residualization of the radioactive metal atom that will be specifically delivered to the cancer cell by the BBN[7–14]NH_2 moiety targeting vector (*28*). Studies with BBN[7–14]NH_2 conjugates radiolabeled with ^{105}Rh, ^{99m}Tc, and ^{111}In have demonstrated receptor-mediated trapping of these radiotracers by GRP-receptor–expressing cancer cells (*14,22,24*). These results demonstrate the feasibility of producing BBN[7–14]NH_2 analogs labeled with a variety of radiometals that hold potential for effective in vivo targeting of GRP-receptor cancer cells.

A fundamental concern in the design of radiometallated peptide constructs is to ensure in vivo stability of the radiometal incorporated by the ligand framework. In vivo stability can be controlled by virtue of the high thermodynamic stability and the kinetic inertness of a specific metal chelation framework (*29–33*). Because the dodecanetetraacetic acid (DOTA) macrocyclic ligand system is well known to form kinetically inert and thermodynamically stable chelates with indium, yttrium, and lanthanides, it has received wide acceptance for in vivo applications with several trivalent radiometals (*29–33*). Our research group is currently evaluating the potential of DOTA-BBN analogs labeled with trivalent radioactive metals, which are linked either directly to the N-terminal amine group of BBN[7–14]NH_2 moiety or through hydrocarbon spacer groups, to specifically target GRP-receptor–expressing cancer cells (Fig. 1) (*18*). The length and composition of the spacer group, or tether, as well as the physicochemical properties of the radiolabeled moiety will influence the GRP-receptor–binding affinity, residualization of radioactivity in cancer cells, and pharmacokinetics of the BBN conjugate. The purpose of this study was to determine the effects of varying the length of the hydrocarbon spacer on the in vitro binding affinity of $^{111}In^{+3}$–DOTA conjugates of BBN[7–14]NH_2 with GRP receptors expressed on PC-3 androgen-independent human prostate cancer cells and their in vivo pharmacokinetics in CF-1 mice. The ultimate goal was identification of one or more lead candidates with optimum in vivo pharmacokinetics and high GRP-receptor–mediated uptake in tumor cells.

MATERIALS AND METHODS

Reagents and Apparatus

All chemicals were obtained from either Aldrich Chemicals or Fisher Scientific, and all chemicals and solvents were reagent grade and used without further purification. The Rink amide 4-methylbenzhydrylamine (MBHA) resin and 9-fluorenylmethyl chloroformate (Fmoc)–protected amino acids were purchased from Calbiochem-Novabiochem Corp., and the other peptide reagents, from Applied Biosystems, Inc. The DOTA-tris(*t*-butyl ester) was purchased from Macrocyclics, and the Fmoc-protected ω-amino alkyl carboxylic acids, from Advanced ChemTech. ^{125}I-Tyr^4-BBN was obtained from NEN Life Sciences Products, Inc., $^{111}InCl_3$ was obtained from Mallinckrodt Medical, Inc., as a 0.05N HCl solution. Electrospray mass spectral analyses were performed by Synpep Corp. PC-3 cells were obtained from American Type Culture Collection and were maintained and grown in the University of

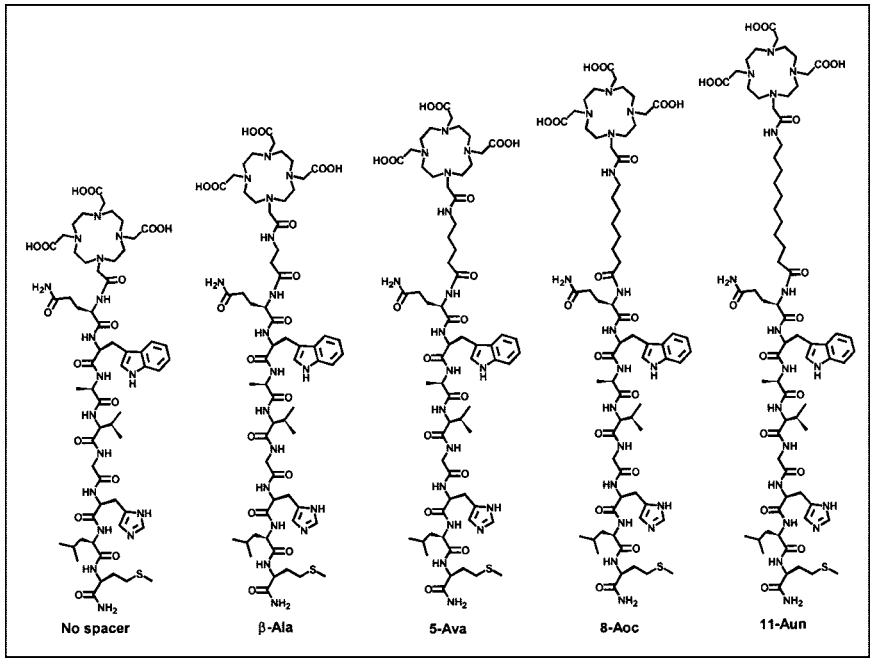

FIGURE 1. DOTA-X-BBN[7–14]NH_2 analogs.

Missouri Cell and Immunobiology Core Facility. CF-1 mice were purchased from Charles River Laboratories and were maintained in an in-house animal facility.

High-Performance Liquid Chromatography (HPLC)

HPLC analyses were performed on a Waters 600E system equipped with a Varian 2550 variable absorption detector, a Packard Radiometric 150TR flow scintillation analyzer, a sodium iodide crystal radiometric detector, an Eppendorf TC-50 column temperature controller, and Hewlett-Packard HP3395 integrators. HPLC solvents consisted of H_2O containing 0.1% trifluoroacetic acid (solvent A) and acetonitrile containing 0.1% trifluoroacetic acid (solvent B). A Phenomenex Jupiter C-18 (5 μm, 300 Å, 4.6 × 250 mm) column was used with a flow rate of 1.5 mL/min. This HPLC gradient system began with an initial solvent composition of 80% A and 20% B followed by a linear gradient to 70% A and 30% B in 30 min, after which the column was reequilibrated.

Solid-Phase Peptide Synthesis

DOTA-X-BBN[7–14]NH_2 conjugates (Fig. 1) were synthesized on a Perkin Elmer–Applied Biosystems model 432 automated peptide synthesizer using traditional Fmoc chemistry, with 2-(1-H-benzotriazole-1-yl)-1,1,3,3-tetramethyluronium hexafluorophosphate activation of carboxyl groups on the reactant, and with the N-terminal amino group on the growing peptide anchored through the C-terminus to the resin. Rink amide MBHA resin (25 μmol), Fmoc-protected amino acids with appropriate side-chain protections (75 μmol), Fmoc-protected ω-amino alkyl carboxylic acids (75 μmol), and DOTA-tris(*t*-butyl ester) (75 μmol) were used for the synthesis. The final products were cleaved by a standard procedure using a cocktail containing thioanisole, water, ethane dithiol, and trifluoroacetic acid in a ratio of 2:1:1:36 and were precipitated into methyl-*t*-butyl ether. Typical yields of the crude peptides were 80%–85%. Crude peptides were purified by HPLC, and the solvents were removed on a SpeedVac concentrator (Thermo Savant). The purified peptides were characterized by electrospray mass spectrometry (Table 1).

In^{+3} Metallation and ^{111}In Labeling

A solution of each DOTA-X-BBN[7–14]NH_2 conjugate (5.0 mg) in 0.2 mol/L tetramethylammonium acetate (0.5 mL) was added to indium chloride (10.0 mg). The pH of the reaction mixture was adjusted to 5.8. The reaction mixture was incubated for 1 h at 80°C (Fig. 2). The resultant In-DOTA-X-BBN[7–14]NH_2 conjugate was purified by reversed-phase HPLC and was analyzed by electrospray mass spectrometry. The results of mass spectral analysis are shown in Table 1. The pure product was obtained as a white powder with a typical yield of 50%–60%.

For ^{111}In labeling, an aliquot of $^{111}InCl_3$ (37 MBq, 50 μL) was added to a solution of DOTA-X-BBN[7–14]NH_2 (100 μg) in 0.2 mol/L tetramethylammonium acetate (500 μL). The pH of the reaction mixture was adjusted to 5.8. The reaction mixture was incubated for 1 h at 80°C. An aliquot of 0.002 mol/L ethylenediaminetetraacetic acid (50 μL) was added to the reaction mixture to complex the unreacted $^{111}In^{+3}$ (Fig. 2). The resultant ^{111}In-DOTA-X-BBN[7–14]NH_2 conjugate was obtained as a single product and was purified by reversed-phase HPLC (Fig. 3). The purified ^{111}In-DOTA-X-BBN[7–14]NH_2 conjugate (27.8–29.6 MBq, 75%–80% recovery) was then concentrated by being passed through an Empore C18-HD high-performance extraction disk (7 mm/3 mL) cartridge and being eluted with 33% ethanol in 0.1 mol/L NaH_2PO_4 buffer (400 μL). The concentrated fraction was then diluted with 0.1 mol/L NaH_2PO_4 buffer (2.3 mL, pH 7) to make the final concentration of ethanol in the solution < 5%.

In Vitro Competitive Cell-Binding, Internalization, and Efflux Studies

The inhibitory concentration of 50% (IC_{50}) of In-DOTA-X-BBN[7–14]NH_2 conjugates was determined by a competitive displacement cell-binding assay using ^{125}I-Tyr^4-BBN. Briefly, 3×10^4 PC-3 cells suspended in Roswell Park Memorial Institute (RPMI) medium 1640 at pH 7.4 and containing 4.8 mg/mL *N*-(2-hydroxyethyl)piperazine-*N*′-(2-ethanesulfonic acid) (HEPES), 0.1 μg/mL Bacitracin (Pharmacia and Upjohn Co.), and 2 mg/mL

TABLE 1
Electrospray Mass Spectrometry and HPLC Data

Analog	Electrospray mass spectrometry			HPLC t_r (min)*
	Molecular formula	Calculated	Observed	
DOTA-X-BBN[7–14]NH_2				
No spacer	$C_{59}H_{91}N_{17}O_{16}S$	1,326.5	1,326.6	13.2
β-Ala	$C_{62}H_{96}N_{18}O_{17}S$	1,397.6	1,397.4	13.4
5-Ava	$C_{64}H_{100}N_{18}O_{17}S$	1,425.7	1,425.8	14.0
8-Aoc	$C_{67}H_{106}N_{18}O_{17}S$	1,467.8	1,467.8	19.1
11-Aun	$C_{70}H_{112}N_{18}O_{17}S$	1,509.8	1,509.8	17.1†
In-DOTA-X-BBN[7–14]NH_2				
No spacer	$C_{59}H_{88}N_{17}O_{16}SIn$	1,438.3	1,438.2	12.9
β-Ala	$C_{62}H_{93}N_{18}O_{17}SIn$	1,509.4	1,509.6	12.7
5-Ava	$C_{64}H_{97}N_{18}O_{17}SIn$	1,536.5	1,537.7	13.6
8-Aoc	$C_{67}H_{103}N_{18}O_{17}SIn$	1,579.6	1,579.7	19.0
11-Aun	$C_{70}H_{109}N_{18}O_{17}SIn$	1,621.6	1,621.7	16.8†

*Used HPLC gradient system as described in Materials and Methods.

†HPLC gradient system begins with initial solvent composition of 70% A and 30% B followed by linear gradient to 50% A:50% B in 30 min, after which column is reequilibrated.

t_r = retention time.

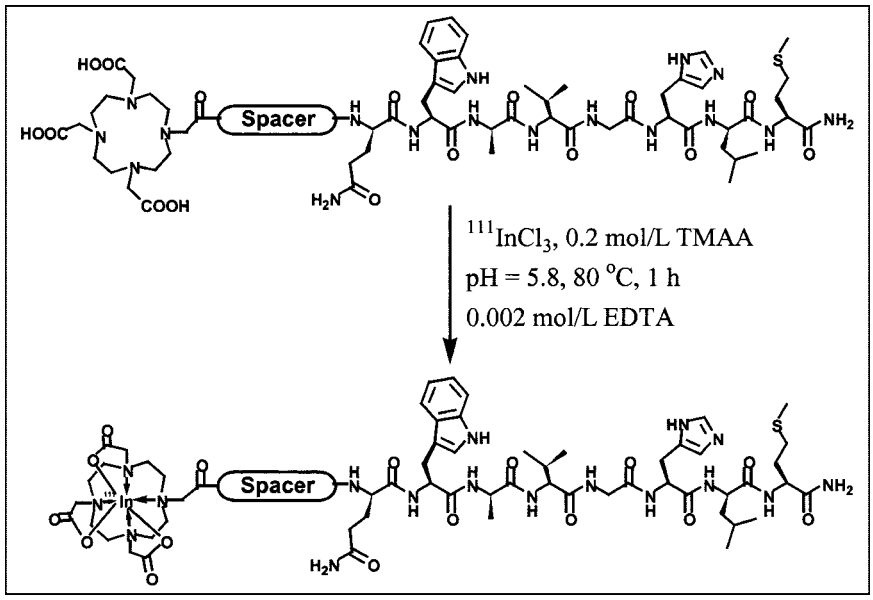

FIGURE 2. Scheme for ^{111}In labeling of DOTA-X-BBN[7–14]NH_2 conjugates. EDTA = ethylenediaminetetraacetic acid.

bovine serum albumin (BSA) were incubated at 37°C and in 5% CO_2 for 40 min in the presence of ^{125}I-Tyr^4-BBN (20,000 cpm, 370 Bq) and increasing concentrations of the In-DOTA-X-BBN[7–14]NH_2 conjugates. After the incubation, the reaction medium was aspirated and the cells were washed 3 times with medium. The radioactivity bound to the cells was counted in a Packard Riastar γ-counting system. The percentage of ^{125}I-Tyr^4-BBN bound to cells was plotted versus increasing concentrations of In-DOTA-X-BBN[7–14]NH_2 conjugates to determine the respective IC_{50} values.

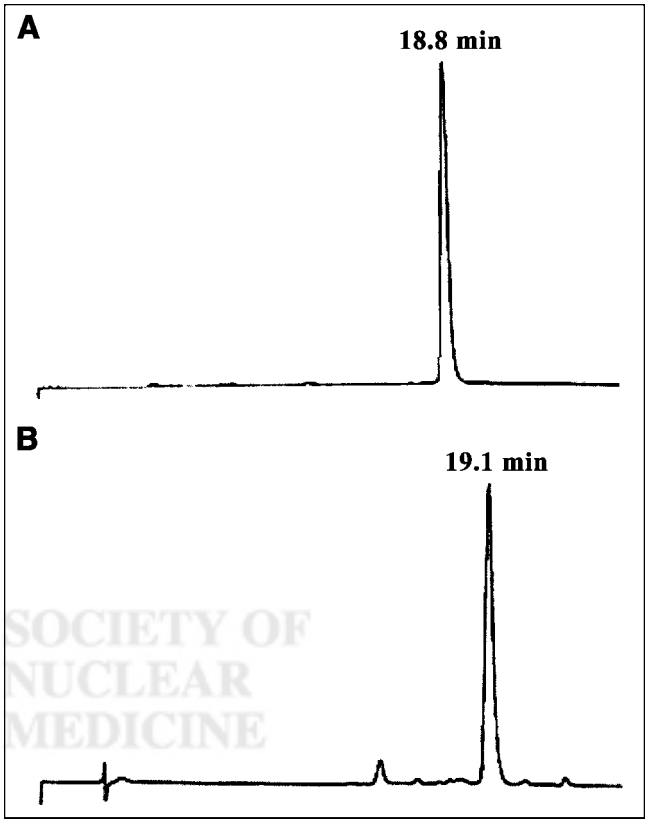

FIGURE 3. HPLC chromatograms of purified ^{111}In-DOTA-8-Aoc-BBN[7–14]NH_2 (radiometric detector) (A) and DOTA-8-Aoc-BBN[7–14]NH_2 (ultraviolet detector at λ = 280 nm) (B).

In vitro studies to determine the degree of internalization of ^{111}In-DOTA-8-Aoc-BBN[7–14]NH_2 conjugate were performed by a method similar to that described by Reile et al. (*9*). These studies were performed by incubating 3×10^4 PC-3 cells (suspended in RPMI medium 1640, at pH 7.4, and containing 4.8 mg/mL HEPES, 0.1 μg/mL Bacitracin, and 2 mg/mL BSA) for 40 min at 37°C and in 5% CO_2 in the presence of 20,000 cpm ^{111}In-DOTA-8-Aoc-BBN[7–14]NH_2 conjugate. After 40 min of incubation, the binding was stopped through aspiration of the reaction medium and washing of the cells with culture medium. The radioactivity-bound cells were then incubated in culture medium at 37°C. After 1, 2, 3, and 4 h of incubation in culture medium, the percentage of radioactivity trapped in the cells was determined after removal of activity bound to the surface of the cells by washing with a pH 2.5 (0.2 mol/L acetic acid and 0.5 mol/L NaCl) buffer.

In Vivo Biodistribution Studies

The biodistribution and uptake of ^{111}In-DOTA-X-BBN[7–14]NH_2 conjugates in healthy CF-1 mice was studied. Each mouse (average weight, 25 g) was injected with an aliquot (50–100 μL) of the HPLC-purified radiolabeled peptide solution (55–75 kBq) through the tail vein. Tissues and organs were excised from the animals sacrificed at 1 h after injection. The activity was counted in a NaI counter, and the percentage injected dose (%ID) per organ and per gram was calculated. The %ID in the blood was estimated assuming a blood volume equal to 6.5% of the total body weight. Receptor-blocking studies were also performed when excess (100 μg) BBN was administered to animals along with the ^{111}In-DOTA-8-Aoc-BBN[7–14]NH_2 conjugate.

Pharmacokinetic Studies of the ^{111}In-DOTA-8-Aoc-BBN[7–14]NH_2 Analog in PC-3 Tumor–Bearing SCID Mice

Four- to 5-wk-old female ICR SCID (severely compromised immunodeficient) outbred mice were obtained from Taconic. Five

mice were housed per sterile Microisolator cage (Alternative Design) in a temperature- and humidity-controlled room with a daily schedule of 12 h of light followed by 12 h of darkness. The animals were fed autoclaved rodent chow (Ralston Purina Co.) and water ad libitum. They were housed for 1 wk before inoculation of tumor cells, and they were anesthetized for injections with isoflurane (Baxter Healthcare Corp.) at a rate of 2.5% with 0.4 L oxygen through a nonrebreathing anesthesia vaporizer.

PC-3 cells were injected bilaterally and subcutaneously in the flank, with $\sim 5 \times 10^6$ cells in a suspension of 100 μL normal sterile saline injected per site. The PC-3 cells were allowed to grow in vivo for 2–3 wk after inoculation, and tumors ranging from 0.2 to 1.0 g developed. The pharmacokinetic studies of the ^{111}In-DOTA-8-Aoc-BBN[7–14]NH_2 conjugate were determined in SCID mice bearing PC-3 tumors. Each mouse (average weight, 25 g) was injected with an aliquot (50–100 μL) of the HPLC-purified ^{111}In-labeled peptide solution (55–75 kBq) through the tail vein. The mice were euthanized, and tissues and organs were excised at 15 min; 30 min; and 1, 4, 24, 48, and 72 h after injection. Subsequently, the tissues and organs were weighed and counted in a NaI well counter, and the %ID and %ID/g of each organ or tissue were calculated. The %ID in whole blood was estimated assuming a whole-blood volume of 6.5% of the total body weight. Receptor-blocking studies were also performed when excess (100 μg) BBN was administered to the animals along with the ^{111}In-DOTA-8-Aoc-BBN[7–14]NH_2 conjugate. All studies were conducted in accordance with protocols approved by the institutional animal care and use committee.

RESULTS

A series of DOTA-X-BBN[7–14]NH_2 (X = 0, β-Ala, 5-Ava, 8-Aoc, or 11-Aun) analogs containing no spacer (0) and 3, 5, 8, and 11 carbon chain spacers was synthesized by solid-phase peptide synthesis using traditional Fmoc chemistry (Fig. 1). The metallation of the DOTA-X-BBN[7–14]NH_2 analogs with both radioactive indium ($^{111}InCl_3$) and nonradioactive indium ($InCl_3$) was performed using the conditions described in Figure 2. The ^{111}In-DOTA-X-BBN[7–14]NH_2 conjugates were obtained in 90%–95% radiochemical yields as single products. The ^{111}In-DOTA-X-BBN[7–14]NH_2 analogs were purified by reversed-phase HPLC before in vivo studies in order to remove corresponding excess nonmetallated DOTA-X-BBN[7–14]NH_2 and obtain the high-specific-activity no-carrier-added ^{111}In-DOTA-X-BBN[7–14]NH_2 conjugates (Fig. 3). All the new DOTA-X-BBN[7–14]NH_2 analogs and their nonradioactive indium complexes were purified by reversed-phase HPLC and characterized by electrospray mass spectrometry (Table 1).

TABLE 2
IC_{50} Values of In-DOTA-X-BBN[7–14]NH_2 Analogs vs. ^{125}I-Tyr^4-BBN in Human Prostate PC-3 Cells

Analog	IC_{50}* (nmol/L)
In-DOTA-BBN[7–14]NH_2	110.6 ± 32.3
In-DOTA-β-Ala-BBN[7–14]NH_2	2.1 ± 0.3
In-DOTA-5-Ava-BBN[7–14]NH_2	1.7 ± 0.4
In-DOTA-8-Aoc-BBN[7–14]NH_2	0.6 ± 0.1
In-DOTA-11-Aun-BBN[7–14]NH_2	64.0 ± 11.2

*n = 3 or 4 separate experiments performed in duplicate.

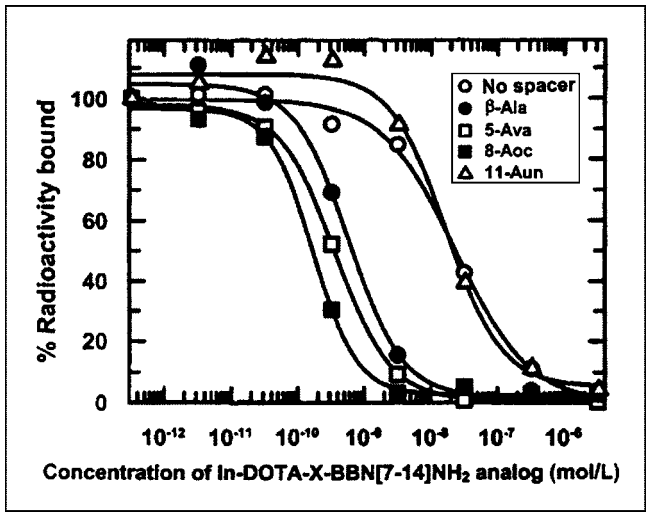

FIGURE 4. Competitive binding assay of In-DOTA-X-BBN[7–14]NH_2 analogs vs. ^{125}I-Tyr^4-BBN in PC-3 cells.

In vitro competitive cell-binding assays performed on PC-3 cells for the In-DOTA-X-BBN[7–14]NH_2 analogs against ^{125}I-Tyr^4-BBN demonstrated a high specificity and affinity (i.e., $IC_{50} < 2.5$ nmol/L; Table 2 and Fig. 4) for the analogs in which the spacer contains 3–8 carbon atoms.

Incubation of the ^{111}In-DOTA-8-Aoc-BBN[7–14]NH_2 analog with PC-3 cells demonstrated rapid internalization of the radioactivity, with measurable surface bound and internalized fractions (Fig. 5). The total residual radioactivity remained almost constant for more than 2 h (Fig. 6). Stability of the ^{111}In-DOTA-8-Aoc-BBN[7–14]NH_2 conjugate showed a human serum half-life of 17.3 h.

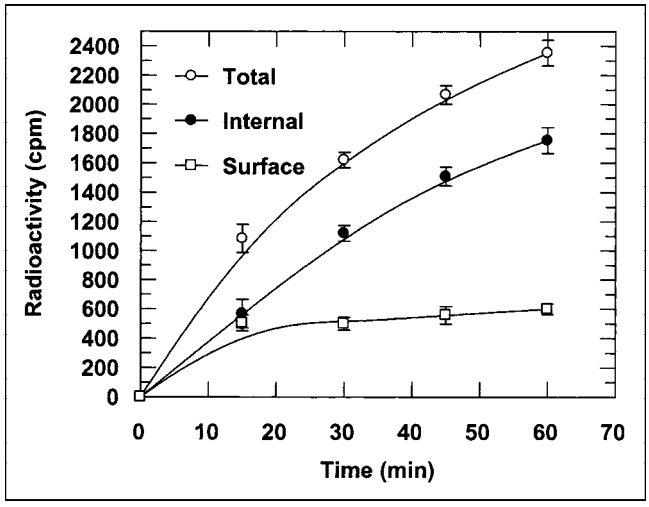

FIGURE 5. Internalization of ^{111}In-DOTA-8-Aoc-BBN[7–14]NH_2 in PC-3 cells (n = 5).

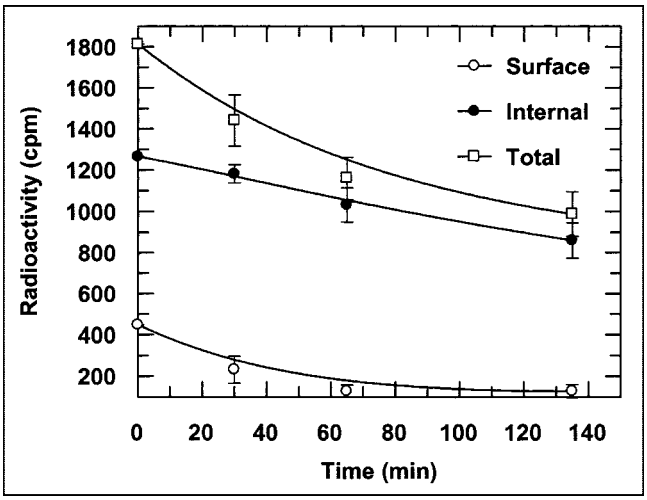

FIGURE 6. Efflux of ^{111}In-DOTA-8-Aoc-BBN[7–14]NH_2 in PC-3 cells (n = 5).

Results from in vivo biodistribution studies of the ^{111}In-DOTA-X-BBN[7–14]NH_2 analogs performed on healthy CF-1 mice at 1 h after injection are summarized in Table 3. All ^{111}In-DOTA-X-BBN[7–14]NH_2 conjugates cleared efficiently from the blood, with the primary route of radioactivity clearance being renal/urinary. Uptake of radioactivity in the pancreas increased as the lipophilicity of the conjugate increased; the value was 0.20 ± 0.04 %ID/g at 1 h after injection. Studies in which 100 μg of BBN were coadministered with the ^{111}In-DOTA-8-Aoc-BBN[7–14]NH_2 conjugate blocked nearly 98% of the pancreatic uptake.

The results from in vivo pharmacokinetic studies for the analog containing 8-Aoc spacer in PC-3 tumor–bearing SCID mice are summarized in Table 4. The radioactivity cleared efficiently from the bloodstream within 1 h after injection. Most of the activity was excreted through the renal/urinary pathway. A tumor uptake of 3.63 ± 1.11 %ID/g was observed at 1 h after injection, and retention over time was significant. Studies in which 100 μg of BBN were coadministered with the ^{111}In-DOTA-8-Aoc-BBN[7–14]NH_2 conjugate blocked approximately 64% of tumor uptake.

DISCUSSION

There are 2 reasons for selecting carbon chain spacers in the DOTA-X-BBN[7–14]NH_2 conjugates. First, these spacers will position the DOTA chelate sufficiently far from the GRP-receptor–binding region of BBN to prevent impedance of the binding affinity of the BBN[8–14]NH_2 motif with GRP receptors, and second, these spacers will optimize pharmacokinetic properties by fine-tuning the lipophilicity of the DOTA-X-BBN[7–14]NH_2 conjugate.

The biologic activity of the DOTA-X-BBN[7–14]NH_2 analogs was determined through in vitro competitive cell-binding assays on PC-3 cells against ^{125}I-Tyr^4-BBN. Results from these cell-binding studies demonstrated that the In-DOTA-X-BBN[7–14]NH_2 analogs containing β-Ala, 5-Ava, and 8-Aoc spacers bind to the GRP receptors on PC-3 cells with high specificity and affinity (i.e., $IC_{50} < 2.5$ nmol/L; Table 2 and Fig. 4). The In-DOTA-X-BBN[7–14]NH_2 analogs containing no spacer and 11-Aun spacer exhibited high GRP-receptor specificity, but the affinity was more than 100-fold less than that of the 8-carbon-spacer analog (Table 2 and Fig. 4). These results were consistent with those obtained in our previous studies with ^{105}Rh-S_4-X-BBN[7–14]NH_2 and ^{99m}Tc-N_3S-X-BBN[7–14]NH_2 conjugates—studies showing that increasing the hydrophobicity of the linker group to excessive levels will reduce the receptor-binding affinity (*14,16,17*). These cell-binding studies indicated that analogs of this design with β-Ala, 5-Ava, and 8-Aoc spacers have a dissociation constant suitable for further in vivo targeting studies of cells expressing GRP receptors.

For optimizing the diagnostic and therapeutic efficacy of a radioactive drug, it is important that the radioactivity be

TABLE 3
^{111}In-DOTA-X-BBN[7–14]NH_2 Analog Biodistribution in CF1 Normal Mice at 1 Hour After Injection

Analog tissue	No spacer	β-Ala	5-Ava	8-Aoc	8-Aoc blocking	11-Aun
Blood	0.10 ± 0.03	0.11 ± 0.06	0.20 ± 0.07	0.32 ± 0.09	0.49 ± 0.15	0.34 ± 0.08
Heart	0.05 ± 0.02	0.06 ± 0.04	0.10 ± 0.04	0.05 ± 0.02	0.16 ± 0.06	0.13 ± 0.04
Lung	0.13 ± 0.03	0.11 ± 0.08	0.20 ± 0.06	0.31 ± 0.07	0.74 ± 0.17	0.26 ± 0.05
Liver	0.09 + 0.01	0.11 + 0.02	0.16 + 0.02	0.65 + 0.07	0.54 + 0.13	1.22 + 0.25
Spleen	0.08 ± 0.02	0.37 ± 0.06	0.87 ± 0.28	1.51 ± 0.41	0.15 ± 0.16	1.15 ± 0.38
Stomach	0.06 ± 0.03	0.30 ± 0.07	0.71 ± 0.24	1.02 ± 0.26	0.32 ± 0.34	1.05 ± 0.25
Large intestine	0.09 ± 0.03	1.10 ± 0.78	3.07 ± 0.86	2.66 ± 1.07	0.16 ± 0.06	4.34 ± 1.34
Small intestine	0.44 ± 0.64	1.01 ± 0.37	3.49 ± 0.87	4.43 ± 0.90	0.95 ± 0.18	11.12 ± 2.07
Kidney	1.24 ± 0.14	1.40 ± 0.27	1.84 ± 0.44	2.37 ± 0.31	2.19 ± 0.47	2.06 ± 0.31
Muscle	0.03 ± 0.02	0.03 ± 0.02	0.05 ± 0.02	0.12 ± 0.05	0.11 ± 0.07	0.09 ± 0.03
Pancreas	0.20 ± 0.04	4.92 ± 0.37	15.78 ± 2.54	26.97 ± 3.97	0.43 ± 0.10	26.00 ± 3.46
Urine (%ID)	97.0 ± 0.4	92.4 ± 0.9	81.3 ± 1.3	71.6 ± 1.8	88.2 ± 1.8	53.3 ± 0.9

Data are %ID/g; n = 5.

TABLE 4
Pharmacokinetics of ^{111}In-DOTA-8-Aoc-BBN[7–14]NH_2 Analog in PC-3 Tumor–Bearing SCID Mice

Tissue	15 min	30 min	1 h	1 h blocking	4 h	24 h	48 h	72 h
Blood	5.59 ± 2.43	1.46 ± 0.44	0.60 ± 0.39	0.68 ± 0.19	0.27 ± 0.02	0.10 ± 0.03	0.07 ± 0.03	0.01 ± 0.02
Heart	2.20 ± 1.05	0.62 ± 0.33	0.25 ± 0.18	0.28 ± 0.17	0.13 ± 0.06	0.05 ± 0.09	0.05 ± 0.05	0.01 ± 0.01
Lung	3.35 ± 1.22	0.94 ± 0.28	0.50 ± 0.39	0.79 ± 0.26	0.25 ± 0.08	0.09 ± 0.07	0.06 ± 0.02	0.02 ± 0.02
Liver	2.03 ± 0.85	0.70 ± 0.21	1.34 ± 0.25	0.79 ± 0.15	1.44 ± 0.57	0.37 ± 0.12	0.13 ± 0.04	0.07 ± 0.02
Spleen	2.21 ± 0.80	0.83 ± 0.26	1.39 ± 1.17	0.21 ± 0.15	1.59 ± 0.27	0.46 ± 0.20	0.22 ± 0.22	0.08 ± 0.09
Stomach	3.30 ± 1.99	1.82 ± 0.44	1.99 ± 0.24	0.34 ± 0.12	0.96 ± 0.57	0.30 ± 0.05	0.12 ± 0.03	0.05 ± 0.02
Large intestine	8.58 ± 3.04	4.33 ± 0.44	4.29 ± 2.55	0.21 ± 0.06	10.30 ± 2.70	2.35 ± 0.43	0.81 ± 0.20	0.45 ± 0.04
Small intestine	7.82 ± 2.26	5.16 ± 1.06	6.80 ± 1.81	2.19 ± 0.43	2.24 ± 0.35	0.89 ± 0.16	0.25 ± 0.06	0.10 ± 0.02
Kidney	29.00 ± 14.40	8.70 ± 2.80	5.66 ± 1.33	3.40 ± 0.62	3.18 ± 0.43	1.18 ± 0.14	0.48 ± 0.09	0.20 ± 0.02
Muscle	1.30 ± 0.60	0.32 ± 0.12	0.08 ± 0.07	0.14 ± 0.10	0.04 ± 0.02	0.05 ± 0.05	0.02 ± 0.04	0.01 ± 0.02
Pancreas	54.30 ± 9.70	27.90 ± 3.40	18.80 ± 11.00	0.46 ± 0.07	16.60 ± 4.40	6.78 ± 1.15	0.77 ± 0.44	0.23 ± 0.08
Tumor	7.59 ± 2.11	4.58 ± 0.53	3.63 ± 1.11	1.32 ± 0.28	1.78 ± 1.09	1.56 ± 0.45	0.68 ± 0.24	0.34 ± 0.10
Urine (%ID)	27.9 ± 10.3	62.6 ± 5.0	68.6 ± 7.0	86.5 ± 1.9	81.8 ± 3.8	87.2 ± 4.3	91.8 ± 4.1	92.5 ± 1.1

Data are average %ID/g; $n = 5$.

residualized in the tumor cell after drug localization at the tumor site (*21*,*22*,*25*,*28*,*34*). Internalization and efflux studies in PC-3 cells were performed with the ^{111}In-DOTA-8-Aoc-BBN[7–14]NH_2 analog, the analog that exhibited the lowest IC_{50} values with PC-3 cell–expressed GRP receptors (Table 2). GRP receptors are 7-TMS-G-protein–coupled receptors that can internalize agonist–receptor complexes (*26*,*27*,*35*). Since the BBN[7–14]NH_2 peptide sequence confers agonistic GRP-receptor–binding capability, the GRP-receptor–mediated endocytosis of the ^{111}In-DOTA-X-BBN[7–14]NH_2 conjugates used in this study was not unexpected. Previous studies with ^{111}In-cycloheximide-B-diethylenetriaminepentaacetic acid-8-Aoc-BBN[7–14]NH_2, ^{105}Rh-S_4-X-BBN[7–14]NH_2, and ^{99m}Tc-N_3S-X-BBN[7–14]NH_2 conjugates also demonstrated GRP-receptor–mediated trapping of radioactivity (*9*,*14*,*16*,*17*). In all these derivatives, the BBN[7–14]NH_2 binding motif was present in the conjugate constructs. The specific intracellular trapping mechanism of the ^{111}In activity in these PC-3 cells is not understood. It is likely that after internalization of ^{111}In-DOTA-8-Aoc-BBN[7–14]NH_2, lysosomal proteases degrade the ^{111}In-DOTA-8-Aoc-BBN[7–14]NH_2 conjugate to peptide fragments (*36*,*37*). The identity of ^{111}In-containing fragments retained by the cell is not known, and further work is needed to identify the structure of the ^{111}In-fragments to help elucidate the trapping mechanisms (*36*,*38*).

In vivo biodistribution studies of the ^{111}In-DOTA-X-BBN[7–14]NH_2 analogs were performed on healthy CF-1 mice. Table 3 summarizes the results of the biodistribution for the ^{111}In-DOTA-X-BBN[7–14]NH_2 analog series on CF-1 mice at 1 h after injection. Because the pancreas is the primary normal tissue in these animals that expresses a high density of bloodstream-accessible GRP receptors, the accumulation of ^{111}In in the pancreas is a direct reflection of the efficacy of radiolabeled BBN analogs for in vivo targeting of cell-surface–expressed GRP receptors (*10*). In the present study, all ^{111}In-DOTA-X-BBN[7–14]NH_2 conjugates cleared efficiently from the blood, with <0.35 %ID/g remaining in the blood at 1 h after injection (Table 3). The primary route of radioactivity clearance from the body is renal/urinary, with more than 70 %ID observed in the urine at 1 h after injection for analogs with no spacer or with the β-Ala, 5-Ava, and 8-Aoc spacers (Table 3). ^{111}In-DOTA-11-Aun-BBN[7–14]NH_2 is cleared to a significantly greater extent through the hepatobiliary route (averaging 26 %ID at 1 h after injection) than are the other derivatives (Table 3); this finding is assumed to be related to the higher lipophilicity of this analog. Retention of radioactivity in the kidneys after administration of all these ^{111}In-DOTA-X-BBN[7–14]NH_2 analogs, at <2.5 %ID/g at 1 h after injection (Table 3), was lower than that of most other small peptide–based radioactive drugs (*32*,*33*,*39*). Uptake of radioactivity in the pancreas increased as the lipophilicity of the conjugate increased; uptake ranged from 0.20 ± 0.04 %ID/g at 1 h after injection for the analog with no spacer (the least lipophilic analog in the series) to 26.97 ± 3.97 %ID/g at 1 h after injection for the analog using the 8-Aoc spacer (second most lipophilic in the series) (Table 3). Biodistribution studies in which an excess (100 μg) of nonradioactive BBN was coinjected with the ^{111}In-DOTA-8-Aoc-BBN[7–14]NH_2 in CF-1 mice demonstrated that uptake in the pancreas is specific and receptor mediated. These studies showed that uptake of this analog was reduced to 0.43 ± 0.10 %ID/g in the pancreas at 1 h after injection (Table 3)—nearly 98% lower than pancreatic uptake of ^{111}In-DOTA-8-Aoc-BBN[7–14]NH_2 when no blocking agent was coinjected (Table 3). The pharmacokinetics and pancreatic accumulation of this short series of ^{111}In-DOTA-X-BBN[7–14]NH_2 analogs indicates that constructs in which the spacer group (X) ranges from 5 to 8 carbon atoms appear to be the most promising for further development as GRP-receptor–targeting radiopharmaceuticals.

On the basis of these observations, we selected the analog containing 8-Aoc spacer for in vivo pharmacokinetic studies on PC-3 tumor–bearing SCID mice. Table 4 summarizes the results of the pharmacokinetic studies on PC-3 tumor–bearing SCID mice. The ^{111}In conjugate cleared efficiently from the bloodstream within 1 h after injection. For example, 0.60 ± 0.39 %ID/g remained in the blood at 1 h after injection. Most of the activity was excreted through the renal/urinary pathway (i.e., 68.6 ± 7.0 %ID at 1 h after injection and 87.2 ± 4.3 %ID at 24 h after injection), with the remainder of the radioactivity being excreted through the hepatobiliary pathway. Receptor-mediated tumor targeting of the PC-3–xenografted SCID mice resulted in tumor uptake and retention values of 3.63 ± 1.11, 1.56 ± 0.45, 0.68 ± 0.24, and 0.34 ± 0.10 %ID/g at, respectively, 1, 24, 48, and 72 h residualization (i.e., 43%, 19%, and 9% of the radioactivity in the tumor at 1 h after injection was retained at, respectively, 24, 48, and 72 h after injection). At 1 h after injection, tumor-to-blood and tumor-to-muscle ratios of approximately 6:1 and 45:1 were achieved. Although ^{111}In in the tumor was not optimal, the fact that the half-life of retention was approximately 24 h indicates that the ^{111}In-DOTA-8-Aoc-BBN[7–14]NH_2 conjugate was internalized agonistically. The observation that coadministration of 100 μg of BBN along with the ^{111}In-DOTA-8-Aoc-BBN[7–14]NH_2 conjugate blocked about 98% of the receptor-mediated radioactivity uptake in pancreas but only 64% in tumor may be related to the fact that these human tumors are supported by murine vasculature architecture (Table 4). Student *t* tests of blocked-versus-unblocked in vivo tumor uptake showed a *t* value of 4.67 and a *P* value of 0.002, indicating a statistical difference among datasets. Accumulation of activity in the kidneys was significant (i.e., 5.66 ± 1.33 %ID/g at 1 h); however, the level of activity decreased with time (i.e., to 1.18 ± 0.14 %ID/g at 24 h and 0.48 ± 0.97 %ID/g at 48 h). It may be possible to reduce the initial accumulation of ^{111}In conjugate in the kidney or accelerate its washout by administration of excess lysine or other positively charged molecules (*38*). Accretion of ^{111}In-DOTA-8-Aoc-BBN[7–14]NH_2 in other tissues or organs was minimal.

The DOTA chelator framework can form complexes with a variety of trivalent and divalent radiometals to produce radiolabeled bioconjugates with high in vitro and in vivo stability (*29*,*30*). Radiometallation of the DOTA-X-BBN[7–14]NH_2 analogs with particle-emitting radionuclides available in high specific activities (including $^{90}Y^{+3}$, $^{64}Cu^{+2}$, $^{177}Lu^{+3}$, $^{149}Pm^{+3}$, and $^{166}Ho^{+3}$) should produce GRP-receptor–avid conjugates with potential for therapeutic applications (*31*,*40*).

The results of studies with these ^{111}In-DOTA-X-BBN[7–14]NH_2 constructs can be used as a basis to design potential therapeutic analogs labeled with β-particle–emitting radionuclides. In some cases, substitution of another metal for $^{111}In^{+3}$ may not significantly modify the in vitro and in vivo properties of DOTA bioconjugates (*29*,*33*). However, the physicochemical properties of the appended radiometallated DOTA moieties may be metal specific and can measurably alter the receptor-binding and pharmacokinetic properties of the bioconjugate (*2*,*33*). Clearly, it will be important to formulate DOTA-X-BBN[7–14]NH_2 analogs complexed with therapeutically useful radiometals and to individually evaluate their utility for specific in vivo targeting of GRP-receptor–expressing cancers.

CONCLUSION

The in vitro studies with PC-3 androgen-independent human prostate cancer cells showed that the ^{111}In-DOTA-X-BBN[7–14]NH_2 analogs in which the spacer group (X) is β-Ala, 5-Ava, and 8-Aoc exhibit high binding affinities (i.e., IC_{50} values ranging from 0.6 to 2.4 nmol/L) for GRP receptors. In vivo studies demonstrated that analogs in which X = 5-Ava and 8-Aoc exhibit high specific localization in the pancreas, normal GRP-receptor–expressing tissue, and efficient clearance from the blood primarily through the renal/urinary pathway. The ^{111}In-DOTA-8-Aoc-BBN[7–14]NH_2 analog binds to GRP receptors acting agonistically, resulting in receptor-mediated endocytosis. These results suggest that the ^{111}In-DOTA-X-BBN[7–14]NH_2 construct, in which X = a tether ranging between a 5-carbon and 8-carbon spacer, may form the basis for development of radiometallated diagnostic or therapeutic radiopharmaceuticals for selective in vivo targeting of GRP-receptor–expressing cancers.

ACKNOWLEDGMENTS

This article is the result of work supported with resources and the use of facilities at the Harry S. Truman Memorial VA Hospital and the Departments of Radiology and Internal Medicine of the University of Missouri-Columbia School of Medicine. This work was also funded in part by grant RPG-99-331-01-CDD from the American Cancer Society and grants DHHS-1P20-CA72942 and DHHS-RO1-CA72942 from the National Cancer Institute. The University of Missouri holds a patent on the BBN agonists cited in this article. T.J. Hoffman, G.L. Sieckman, and W.A. Volkert are coinventors in this patent.

REFERENCES

1. Okarvi SM. Recent developments in ^{99m}Tc-labelled peptide-based radiopharmaceuticals: an overview. *Nucl Med Commun.* 1999;20:1093–1112.
2. Hoffman TJ, Quinn TP, Volkert WA. Radiometallated receptor-avid peptide conjugates for specific in vivo targeting of cancer cells. *Nucl Med Biol.* 2001; 28:527–539.
3. Anastasia A, Erspamer V, Bucci H. Isolation and structure of bombesin and alytesin, two analogous active peptides from the skin of the European amphibians Bombina and Alytes. *Experientia.* 1971;27:166–168.
4. Reubi JC, Wenger S, Schmuckli-Maurer J, Schaer J-C, Gugger M. Bombesin receptor subtypes in human cancers: detection with the universal radioligand ^{125}I-[D-Tyr^6, β-Ala^{11}, Phe^{13}, Nle^{14}] bombesin(6–14). *Clin Cancer Res.* 2002;8: 1139–1146.
5. Qin Y, Ertl T, Cai R-Z, Halmos G, Schally AV. Inhibitory effect of bombesin receptor antagonist RC-3095 on the growth of human pancreatic cancer cells in vivo and in vitro. *Cancer Res.* 1994;54:1035–1041.

6. Mahmoud S, Staley J, Taylor J, et al. [Psi[13, 14]] Bombesin analogues inhibit growth of small cell lung cancer in vitro and in vivo. *Life Sci.* 1985;37:105–113.
7. Coy DH, Jensen RT, Jiang NY. Systematic development of bombesin/gastrin-releasing peptide antagonists. *J Natl Cancer Inst Monogr.* 1992;13:133–139.
8. Moody TW. Review: peptides and growth factors in non-small cell lung cancer. *Peptides.* 1996;17:545–555.
9. Reile H, Armatis PE, Schally AV. Characterization of high-affinity receptors for bombesin/gastrin releasing peptide on the human prostate cancer cell lines PC-3 and DU-145: internalization of receptor bound ^{125}I-(Tyr^4)-bombesin by tumor cells. *Prostate.* 1994;25:29–38.
10. Scemama JL, Zahidi A, Fourmy D, et al. Interaction of [^{125}I]-Tyr^4-bombesin with specific receptors on normal human pancreatic membranes. *Regul Pept.* 1986; 13:125–132.
11. Van de Wiele C, Dumont F, Broecke RV, et al. Technetium-99m RP525, a GRP analogue for visualization of GRP receptor-expressing malignancies: a feasibility study. *Eur J Nucl Med.* 2000;27:1694–1699.
12. Hoffman TJ, Sieckman GL, Volkert WA. Targeting small cell lung cancer using iodinated peptide analogues. *J Labelled Compds Radiopharm.* 1995;37:321–325.
13. Hoffman TJ, Sieckman GL, Volkert WA. Iodinated bombesin analogs: effect of a N-terminal vs. side chain iodine attachment of BBN/GRP receptor binding [abstract]. *J Nucl Med.* 1996;37(suppl):185P.
14. Hoffman TJ, Li N, Volkert WA, Sieckman GL, Higginbotham C, Ochrymowcycz LA. Synthesis and characterization of ^{105}Rh labeled bombesin analogues: enhancement of GRP receptor binding affinity utilizing aliphatic carbon chain linkers. *J Labelled Compds Radiopharm.* 1997;40:490–493.
15. Karra SR, Schibli R, Gali H, et al. ^{99m}Tc labelling and in vivo studies of a bombesin analog with a novel water-soluble bifunctional chelating agent. *Bioconjug Chem.* 1999;10:254–260.
16. Hoffman TJ, Simpson SD, Smith CJ, et al. Accumulation and retention of Tc-99m RP527 by GRP receptor expressing tumors in scid mice [abstract]. *J Nucl Med.* 1999;40(suppl):104P.
17. Hoffman TJ, Smith CJ, Simpson SD, et al. Optimizing pharmacokinetics of ^{99m}Tc-GRP receptor targeting peptides using multi-amino acid linking groups [abstract]. *J Nucl Med.* 2000;41(suppl):228P.
18. Smith CJ, Hoffman TJ, Hayes DL, Owen NK, Sieckman GL, Volkert WA. Radiochemical investigations of ^{177}Lu-DOTA-8-Aoc-BBN[7–14]NH_2: a new gastrin releasing peptide receptor (GRPr) targeting radiopharmaceutical. *J Labelled Compds Radiopharm.* 2001;44(suppl):706–708.
19. Safavy A, Khazaeli MB, Qin H, Buchsbaum DJ. Synthesis of bombesin analogues for radiolabeling with rhenium-188. *Cancer Suppl.* 1997;80:2354–2359.
20. Baidoo KE, Lin KS, Zhan Y, Finley P, Scheffel U, Wagner HN Jr. Design, synthesis, and initial evaluation of high-affinity technetium bombesin analogues. *Bioconjug Chem.* 1998;9:218–225.
21. Breeman WAP, Hofland LJ, DeJong M, et al. Evaluation of radiolabelled bombesin analogues for receptor-targeted scintigraphy and radiotherapy. *Int J Cancer.* 1999;81:658–665.
22. Breeman WAP, De Jong M, Bernard BF, et al. Pre-clinical evaluation of [^{111}In-DTPA-Pro^1, Tyr^4]bombesin, a new radioligand for bombesin-receptor scintigraphy. *Int J Cancer.* 1999;83:657–663.
23. Lin KS, Baidoo KE, Hashemzadeh-Gargari H, Wagner HN. A new high affinity hydrophilic ^{99m}Tc-diaminedithiol analog of bombesin [abstract]. *J Nucl Med.* 2000;41(suppl):40P.
24. Rogers BE, McCarthy DW, Sharp TL, et al. Evaluation of a ^{64}Cu-labeled bombesin analogue for diagnosis of gastrin-releasing peptide receptor positive tumors by microPET imaging. *J Labelled Compds Radiopharm.* 2001;44(suppl): S81–S83.
25. Bijsterbosch MK. Selective drug delivery by means of receptor-mediated endocytosis. *Q J Nucl Med.* 1995;39:4–9.
26. Fraser CM. Structural and functional analysis of G protein-coupled receptors and potential diagnostic ligands. *J Nucl Med.* 1995;36(suppl):17S–21S.
27. Harden TK, Boyer JL, Dougherty RW. Drug analysis based on signaling responses to G-protein-coupled receptors. In: Leff P, ed. *Receptor-Based Drug Design.* New York, NY: Marcel Dekker, Inc; 1998:79–105.
28. Behr TM, Goldenberg DM. Improved prospects for cancer therapy with radiolabeled antibody fragments and peptides. *J Nucl Med.* 1996;37:834–836.
29. Liu S, Edwards DS. Bifunctional chelators for therapeutic lanthanide radiopharmaceuticals. *Bioconjug Chem.* 2001;12:7–34.
30. Li M, Meares CF, Zhong GR, Miers L, Xiong CY, DeNardo SJ. Labeling monoclonal antibodies with ^{90}yttrium- and ^{111}indium-DOTA chelates: a simple and efficient method. *Bioconjug Chem.* 1994;5:101–104.
31. Cutler CS, Smith CJ, Ehrhardt GJ, Tyler TT, Jurisson SS, Deutsch E. Current and potential therapeutic uses of lanthanide radioisotopes. *Cancer Biother Radiopharm.* 2000;15:531–545.
32. de Jong M, Bakker WH, Krenning EP, et al. Yttrium-90 and indium-111 labelling, receptor binding and biodistribution of [DOTA^0, d-Phe^1, Tyr^3]octreotide, a promising somatostatin analogue for radionuclide therapy. *Eur J Nucl Med.* 1997;24:368–371.
33. Heppeler A, Froidevaux S, Mäcke HR, et al. Radiometal-labelled macrocyclic chelator derivatized somatostatin analogue with superb tumor targeting properties and potential for receptor mediated internal radiotherapy. *Chem Eur J.* 1999;5: 1974–1981.
34. Lister-James J, Moyer BR, Dean RT. Pharmacokinetic considerations in the development of peptide-based imaging agents. *Q J Nucl Med.* 1997;41:111–118.
35. Beck-Sickinger AG. Structural characterization and binding sites of G-protein-coupled receptors. *Drug Discov Today.* 1996;1:502–513.
36. Duncan JR, Welch MJ. Intracellular metabolism of indium-111-DTPA-labeled receptor targeted proteins. *J Nucl Med.* 1993;34:1728–1738.
37. Novak-Hofer I, Amstutz HP, Morgenthaler JJ, Schubiger PA. Internalization and degradation of monoclonal antibody chCE7 by human neuroblastoma cells. *Int J Cancer.* 1994;57:427–432.
38. Arano Y. Strategies to reduce renal radioactivity levels of antibody fragments. *Q J Nucl Med.* 1998;42:262–267.
39. Chen J, Chen Z, Hoffman TJ, Jurisson SS, Quinn TP. Melanoma-targeting properties of (99m)technetium-labeled cyclic alpha-melanocyte-stimulating hormone peptide analogues. *Cancer Res.* 2000;60:5649–5658.
40. Volkert WA, Hoffman TJ. Therapeutic radiopharmaceuticals. *Chem Rev.* 1999; 99:2269–2292.